


P2X7 receptor induces microglia polarization to the M1 phenotype in cancer-induced bone pain rat models

Molecular Pain
Volume 18: 1–11
© The Author(s) 2022
Article reuse guidelines:
sagepub.com/journals-permissions
DOI: 10.1177/17448069211060962
journals.sagepub.com/home/mpx


Ping Wu¹, Guohua Zhou², Xiaoqi Wu², Run Lv³, Jiaqi Yao¹, and Qingping Wen¹

Abstract

Background: The transition from pro-inflammatory M1 phenotype to anti-inflammatory M2 phenotype presents a novel therapeutic strategy for chronic pain.

Objective: We investigated the role of microglia polarization in cancer-induced bone pain (CIBP), as well as the role of the P2X7 receptor in modulating M1 to M2 polarization.

Methods: Walker-256 breast cancer cells were administered into tibias of female rats to induce bone cancer-associated cancer.

Results: During bone cancer development, the P2X7 receptor and M1 microglia markers were upregulated. In contrast, inhibition of the P2X7 receptor by BBG, a blood-brain barrier-permeable P2X7R-specific antagonist, alleviated the pain and promoted microglia polarization toward the M2 phenotype, while suppressing the M1 phenotype *in vivo* and *in vitro*.

Conclusion: P2X7 receptor-mediated spinal microglia polarization is involved in alleviation of CIBP. Therefore, P2X7R is a potential option for CIBP treatment.

Keywords

Cancer-induced bone pain, P2X7 receptor, microglia polarization, BV2

Date Received: 5 August 2021; Revised 17 October 2021; accepted: 1 November 2021

Introduction

Cancer-induced bone pain (CIBP) is a severe form of cancer pain that is often managed poorly, thereby significantly compromising the quality of life for patients.¹ Effective pain control is not only important for comprehensive treatment of cancer, but is associated with prolonged patient survival outcomes.² However, the current treatment options for bone pain are limited by their ineffective analgesic properties or inevitable side effects.³ Therefore, there is a need to investigate the pathomechanisms of CIBP, which would form the basis for the development of effective treatment strategies.

Animal models have been used to investigate CIBP pathogenesis as well as to assess the efficacies of potential drugs.⁴ In CIBP models, pain sensation is detected at the

affected hind paw, rather than at the tumor infiltration area.⁵ This is based on the dependence of CIBP to central sensitization.⁶ Microglia is a central resident macrophage that

¹Department of Anesthesiology, The First Affiliated Hospital of Dalian Medical University, Dalian, China

²Anesthesiology Department, Dalian Medical University, Dalian, China

³Department of Anesthesiology, The first hospital of Hebei Medical University, Shijiazhuang, China.

Ping Wu, Guohua Zhou these authors contributed equally to this study.

Corresponding Author:

Qingping Wen, Department of Anesthesiology, The First Affiliated Hospital of Dalian Medical University, No. 222, Zhongshan Road, Dalian 116000, China.

Email: qingping_wen@yahoo.com



Creative Commons Non Commercial CC BY-NC: This article is distributed under the terms of the Creative Commons Attribution-NonCommercial 4.0 License (<https://creativecommons.org/licenses/by-nc/4.0/>) which permits non-commercial use, reproduction and distribution of the work without further permission provided the original work is attributed as specified on the SAGE

and Open Access pages (<https://us.sagepub.com/en-us/nam/open-access-at-sage>).

modulates neuronal sensitization.⁷ In response to stimuli, microglia adopts distinctive phenotypes, the alternative M2 and classical M1 phenotypes. Microglia of the M1 phenotype exhibit elevated levels of CD86 and inducible NO synthase (iNOS).⁸ The shift of microglia to the M1 phenotype initiates the synthesis and secretion of various inflammation-promoting cytokines, including, tumor necrosis factor- α (TNF- α) and interleukin (IL)-18 which activate neighboring neurons, resulting in sensitization and pain persistence.⁹ Besides, the M2 microglia is characterized by increased expression levels of arginase-1 (Arg-1) and CD163, and they secrete inflammation-inhibiting cytokines, such as IL-4 and IL-10. Anti-inflammatory cytokines suppress inflammatory responses and mediate restoration of immune homeostasis.¹⁰ Stimulation of polarization to the M1 phenotype by processes such as intrathecal injection of LPS can cause hypersensitive pain reactions.¹¹ Inhibition of microglial polarization to the M1 state can significantly suppress pain.¹²

The P2X7 receptor (P2X7R) modulates microglial activation.^{13–15} Following CIPB, this receptor is predominantly found in microglia and in the spinal cords.¹⁶ Deletion of the P2RX7 gene was shown to significantly reduce pain hypersensitivity in response to peripheral nerve damage in mice.¹⁷ In ischemia-induced pain models, Higashi et al.¹⁸ found that P2X7R promoted microglial differentiation toward the M1 phenotype, while its inhibition suppressed this differentiation, thereby relieving pain. However, the role of P2X7R in M1/M2 polarization in CIBP has not been clearly elucidated. In this study, we used Walker 256 breast cancer-induced bone pain female rat models to investigate the role of microglial polarization in CIBP. Moreover, we evaluated whether suppression of P2X7R activities can alleviate CIBP by modulating M1 to M2 polarization.

Materials and methods

Experimental animals

Female Sprague-Dawley (SD) rats weighing 180–220 g were purchased from the Institute of Genome Engineered Animal Models for Human Diseases (Dalian, China). Animals were kept in sterile plastic cages under an SPF grade environment at the Dalian Medical University. They were maintained at room temperature ($22 \pm 1^\circ\text{C}$) with a 12 h dark/light cycle, provided with sufficient clean water and food. Animal experiments were permitted by the Ethical Committee on Animal Research of Dalian Medical University.

Cell culture

Culture of cell lines. Walker 256 mammary gland carcinoma cells (donated by Prof. Changsheng Dong (Shanghai Research Institute of Traditional Chinese Medicine, China) were cultured in RPMI 1640 medium enriched with 2% penicillin/streptomycin, 10% fetal bovine serum (FBS), and 1% L-glutamine. Cells were separated from culture flasks using 0.25% trypsin, centrifuged, and reconstituted in PBS.

BV2 Cells. Mouse BV2 cells were bought from Procell Life Science & Technology Co, Ltd (Wuhan, China) and passaged in DMEM:F12 (1:1) medium containing Glutamax, 100 U/mL penicillin and 10% FBS in a humidified atmosphere (37°C , 5% CO_2). At intervals of 2–3 days, the medium was replaced.

CIBP model

We established a CIBP rat model according to a previously described protocol.¹ Briefly, rats were intraperitoneally injected with pentobarbital sodium (50 mg/kg). The CIBP group was administered with 10 μL of walker 256 breast cancer cells (about 5×10^5) in PBS at intramedullary cavity of the left tibia, while the sham group was administered with 10 μL PBS. To prevent cancer cell leakage along the injection track, the syringe was maintained in place for 2 min before removal. The injection was sealed with bone wax while the injection hole was closed in layers and covered with penicillin.

Experimental design

Experiment 1: The CIBP models were evaluated at 7, 14, and 21 days post-implantation of Walker 256 cells. Rats were randomized into Sham group (sacrificed 21 days after PBS injection); CIBP 7 d group (sacrificed 7 days post-implantation of tumor cells); CIBP 14 d group (sacrificed 14 days post-implantation of tumor cells), and CIBP 21 d group (sacrificed 21 days post-implantation of tumor cells). Besides, Paw Withdrawal Thresholds (PWTs) and Number of Spontaneous Flinches (NSFs) were examined, and then, tissues were harvested accordingly (Figure 1(a)).

Experiment 2: The role of P2X7R in CIBP was evaluated by treatment with Brilliant Blue G (BBG), a P2X7R-specific antagonist. Rats were randomized into Sham + NS group, Sham + BBG group, CIBP + NS group, or CIBP + BBG group. Rats in the Sham + BBG and CIBP + BBG groups were intraperitoneally administered with BBG, (APExBIO, C5579) 50 mg/kg from day 7 to day 21, once daily. The dosage was determined from previous literature and subjected to preliminary evaluation.¹⁹ Rats in the Sham + NS and CIBP + NS groups were administered with the same volume of saline solution (Figure 1(b)).

Experiment 3: The BV2 cells were selected as alternatives for investigating microglia *in vitro*. Three different siRNAs targeting mouse P2RX7 gene and a non-targeting siRNA were prepared by Genepharma Co, Ltd (Shanghai, China) (Supplementary File 1). siRNAs targeting P2X7R mRNA and a non-targeting siRNA control were infected using Lipofectamine 2000 (Invitrogen, Carlsbad, CA, USA). Western blot was used to screen siRNAs with the highest silencing efficiency. Then, BV2 cells were assigned into: Control+NCsiRNA group, Control+P2X7RsiRNA group, LPS+BzATP +NCsiRNA group, or LPS+ BzATP +P2X7RsiRNA group (Figure 1(c)).

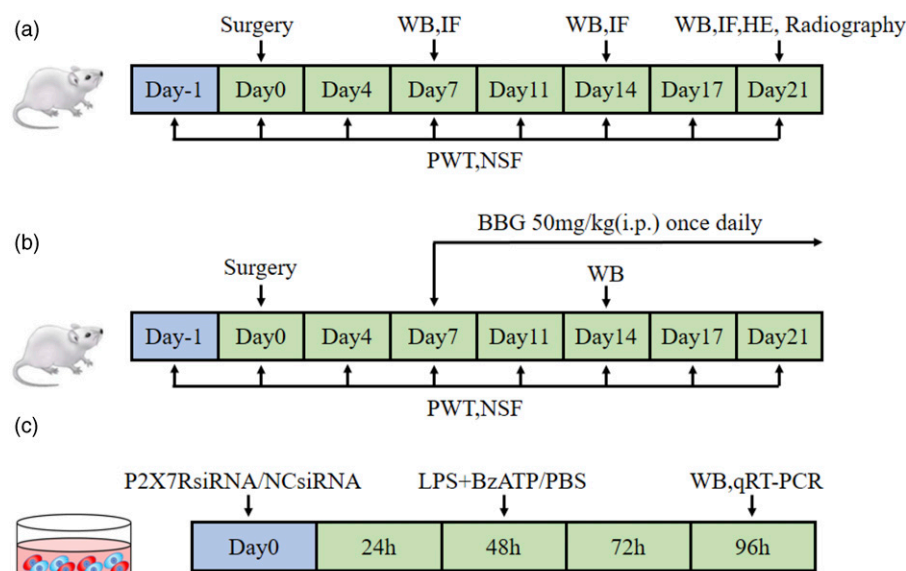


Figure 1. The design of experiment. (a) Experiment 1: Implantation of Walker-256 tumor cells to establish CIBP rat model; (b) Experiment 2: The treatment of CIBP rat model with BBG; (c) Experiment 3: P2X7RsiRNA administration in cultured BV2 cells.

Behavioral assays

Rats were acclimatized to the testing room for 30 min. Spontaneous (flinching guarding and mechanical allodynia) pain features were assessed using PWTs and NSF, respectively. PWTs, following von Frey filament stimulation, were measured as previously described.¹ For the NSF test, rats were left in plexiglass cages and the number of spontaneous withdrawals of the hindlimb on the operated side of the rat within 2 min recorded, which indicated nociceptive behaviors. Each rat was tested 5 times at an interval of 10 min and the average value taken as the final NSF result. These tests were performed 1 day before the operation, and on days 4, 7, 11, 14, 17, and 21 after operation.

A trained specialist, who was blinded to treatment groups, performed all tests.

Radiology

After intraperitoneal anesthetization of rats using sodium pentobarbital, rats were placed in front of an X-ray source (Ray-Nova Pet DR) for imaging the tibia on the operated side. The extent of bone destruction was assessed by two radiologists.

Pathology

HE staining. Rats in the CIBP and Sham groups were euthanized 21 days after modeling, after which their tibias were obtained. After demineralization in 10% EDTA decalcification solution for 2 weeks, tissues were paraffin-embedded and sliced into 4 μ m sections. Slices were kept floating in warm water at 40°C to flatten them, after which they were baked at 60°C in an oven. The degree of tumor invasion was observed in tissues stained with hematoxylin and eosin reagents.

Immunofluorescence assays. Spinal cord specimens were excised from sacrificed rats, fixed in 4% paraformaldehyde for 12–24 h, and embedded in paraffin. Paraffin-embedded samples were sliced into 8 μ m sections for immunofluorescence staining. Briefly, sections were deparaffinized two times in xylene, 15–20 min each, and dehydrated by exposure to pure ethanol at intervals of 10 min after which they were dehydrated in gradient ethanol; 95%, 90%, 80%, and 70% ethanol, for 5 min each. Then, tissues were subjected to antigen retrieval procedures and exposed to 10% donkey serum to block sections at room temperature (RT) for 1 h. This was followed by incubation in the presence of primary antibodies, anti-P2X7R, anti-Iba1, anti-GFAP, and anti-NeuN for 12 h at 4°C. Thereafter, sections were incubated for 50 min in the presence of secondary antibodies at RT in darkness. Finally, they were incubated with anti-DAPI for 10 min at RT in the dark. Spinal cord images were obtained by fluorescence microscopy (NIKON Eclipse Ci, Japan). Antibodies used in this study are shown in [Supplementary Table 1](#).

Western blot analysis

Spinal cord tissues from L4–L6 segments were homogenized to isolate BV2 cells using a lysis buffer containing a protease inhibitor (#R0010, Solarbio, Beijing, CHN). The BCA assay was used to quantify extracted proteins, after which equal amounts of protein were loaded and separated by SDS-PAGE gel electrophoresis. Proteins were electro-transferred to a PVDF membrane and treated with 5% blocking solution at RT for 1 h. Then, the blot was incubated overnight with dilute primary antibodies at 4°C, washed three times in TBST and incubated with a horseradish peroxidase (HRP)-conjugated

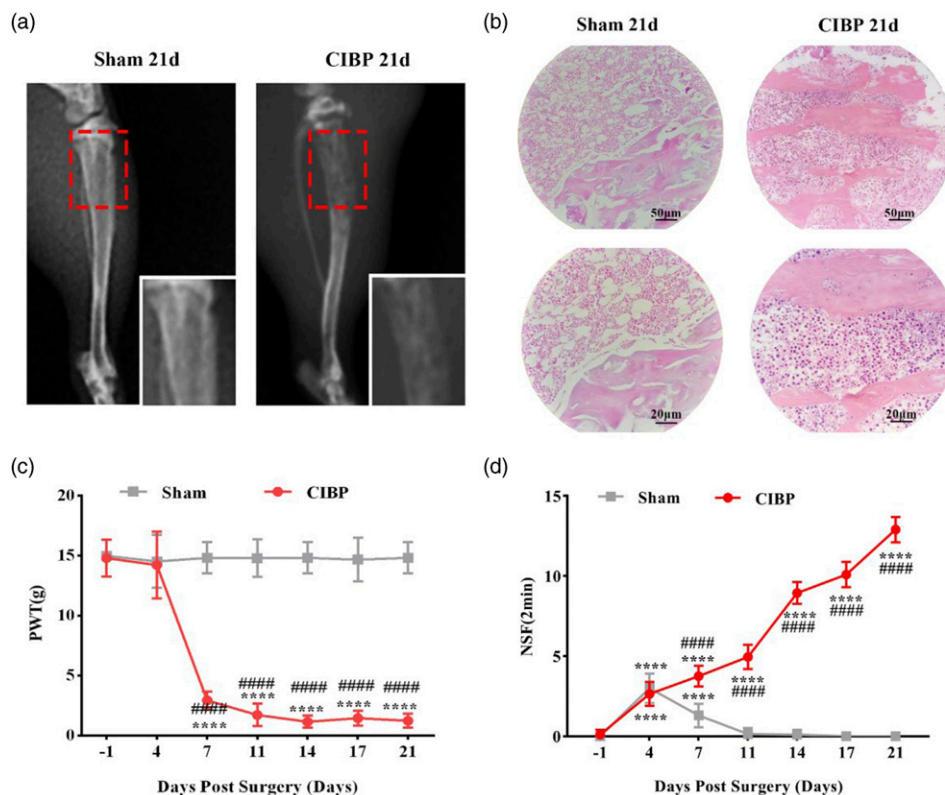


Figure 2. The establishment of breast cancer-induced bone metastasis model in rats. (a) Radiographs of tibia 21 days after Walker 256 cells inoculation. The red frame circled the damage of the proximal cortical bone. (b) 21 days after cancer cells inoculation, hematoxylin-eosin (HE) staining of the proximal cortical bones. The bone marrow spaces are full of malignant tumor cells. (c) Paw withdrawal thresholds (PWTs) were examined on baseline (1 day before surgery) and postoperative days (POD) 4, 7, 11, 14, 17, 21. Data were presented as mean \pm SD ($n = 8$ per group). $***p < .0001$ versus baseline; $####p < .0001$ versus Sham group. (d) Number of Spontaneous Flinches (NSF) was examined on baseline (1 day before surgery) and POD 4, 7, 11, 14, 17, and 21. Data were presented as mean \pm SD ($n = 8$ per group). $***p < .0001$ versus baseline; $####p < .0001$ versus Sham group.

secondary antibody for 2 h at RT. Protein bands were detected using ECL reagents (K-12045-D50, Advansta, USA) and evaluated by the ImageJ software. Antibodies used in this experiment are shown in [Supplementary Table 1](#).

qRT-PCR analysis of mRNA expression levels

Total RNA were extracted from BV2 cells using the Trizol reagent and used to synthesize cDNA using a cDNA Synthesis SuperMix (TransGen Biotech) according to the manufacturer's instructions. Subsequently, a SYBR Select Master Mix (Life Technology) was used to perform q-PCR with corresponding primers ([Supplementary Table 2](#)). The $\Delta\Delta Ct$ method was used to calculate relative fold changes of the expressions of each messenger RNA (mRNA) relative to expressions of GAPDH.

Statistical analysis

Data analyses were performed using GraphPad Prism 8 (GraphPad Software Inc., La Jolla, CA). Normally distributed

data were presented as mean \pm SD. Comparisons of means for two groups were compared using the Student's unpaired t test. Statistical significance was set at $p \leq .05$.

Results

Experimental design

Establishment and assessment of bone metastasis of breast cancer in rat models. Bone metastasis rat models were established by administering Walker 256 mammary gland carcinoma cells directly into the tibia. X-rays and HE staining were used to confirm successful tumor cell implantation. Tibia X-rays obtained on day 21 after intratibial surgery revealed the occurrence of bone destruction and tumor cell infiltration in the CIBP group and complete infiltration of cancer cells into the bone marrow cavity as well as severe damage of the tibia ([Figure 2\(a\)](#)). HE staining showed complete infiltration of tumor cells into the bone marrow cavity of the tibia in the CIBP group and severe damage of bone structures, including to the trabeculae and cortical bone. X-rays and HE

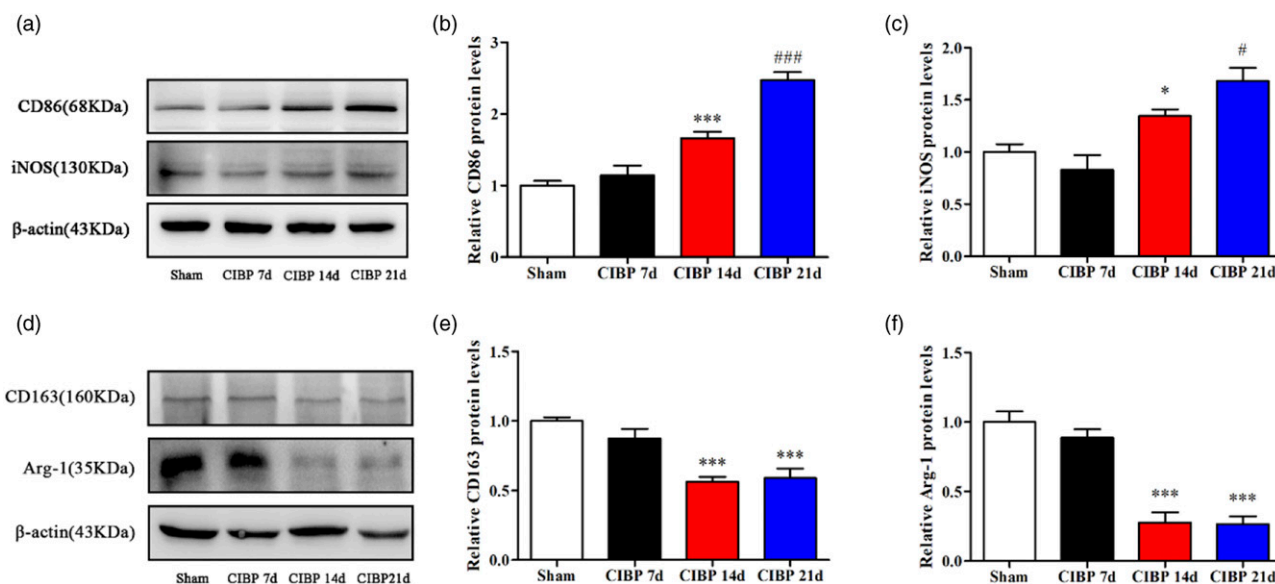


Figure 3. The microglia in the CIBP group polarized toward M1 type. (a), (b), (c) Representative Western blotting bands and quantitative analysis showed that the expression levels of CD86 and iNOS protein in the Sham group and CIBP group on POD 7, 14, 21. β -actin was used as an internal control. Data were presented as mean \pm SD ($n = 4$ per group). * $p < .05$ versus Sham group; # $p < .05$ versus CIBP group on POD 14; *** $p < .001$ versus Sham group; ### $p < .001$ versus CIBP group on POD 14. (d), (e), (f) Representative Western blotting bands and quantitative analysis showed that the expression levels of CD163 and Arg-1 proteins in Sham group and CIBP group on POD 7, 14, and 21. β -actin was used as an internal control. Data were presented as mean \pm SD ($n = 4$ per group). *** $p < .001$ versus Sham group.

results did not however, reveal tibial destruction in the sham group (Figure 2(b)). Animal behavioral hypersensitivities were evaluated from two perspectives. Allodynia in response to mechanical stimulate, which was expressed as PWTs, was significantly decreased on days 7, 11, 14, 17, and 21 after surgery ($p < .05$) in the ipsilateral hind paw of the disease model group, compared to the sham group (Figure 2(c)). Besides, in the Sham group, spontaneous pain behaviors indicated by NSF were transiently increased on day four ($p < .0001$) but subsequently returned to baseline. Moreover, unlike in the sham group, NSF continuously increased from day 4 to day 21 in the CIBP group ($p < .0001$; Figure 2(d)).

Microglia in CIBP models were polarized toward the M1 type

Microglia is resident macrophages in the CNS and is involved in CIBP development.²⁰ The dorsal horn of the spinal cord has been shown to be the main site of central sensitization. To determine whether microglial cells in the L₄₋₆ segment of the spinal cord were polarized toward the M1 type, we used Western blot analysis to assess markers of M1 and M2 types (Figure 3(a) and (d)). On day 21, M1-type markers, CD86 and iNOS, were significantly elevated in CIBP14, while M2-type markers, CD163 and Arg-1, were significantly suppressed ($p < .05$; Figure 3(b), (c), (e), (f)). Therefore, microglia in the CIBP group was polarized toward the M1 type.

P2X7R expressions in the microglia of spinal dorsal horn were upregulated after tumor inoculation

Next, we evaluated various factors that are involved in microglial polarization. First, we assessed the location of P2X7R by double-immunofluorescence staining for P2X7R and Iba-1 (microglial biomarkers), GFAP (astrocyte biomarker), or NeuN (neuron biomarker) on day 14 after surgery. Imaging showed that most P2X7R were co-expressed with Iba-1 positive cells in the ipsilateral spinal dorsal horn, but not with GFAP or NeuN positive cells (Figure 4(a)). Then, we investigated the expression and distribution of P2X7R in the spinal dorsal horn after tumor inoculation by immunofluorescence and Western blot. The levels of P2X7R in the CIBP group were upregulated over time when compared to the Sham group (Figure 4(b) to (e)).

P2X7R inhibition relieved cancer-induced bone pain and promoted microglial polarization toward the M2 type

Through pharmacologic approaches, we evaluated the effects of P2X7R on CIBP pathogenesis. We injected BBG, a P2X7R-specific antagonist with nice blood-brain barrier permeability, i.p. (50 mg/kg). BBG treatment significantly elevated PWTs and suppressed NSF, implying that BBG can effectively alleviate mechanical allodynia and spontaneous pain (Figure 5(a) and (b)). In addition, Western blot assays

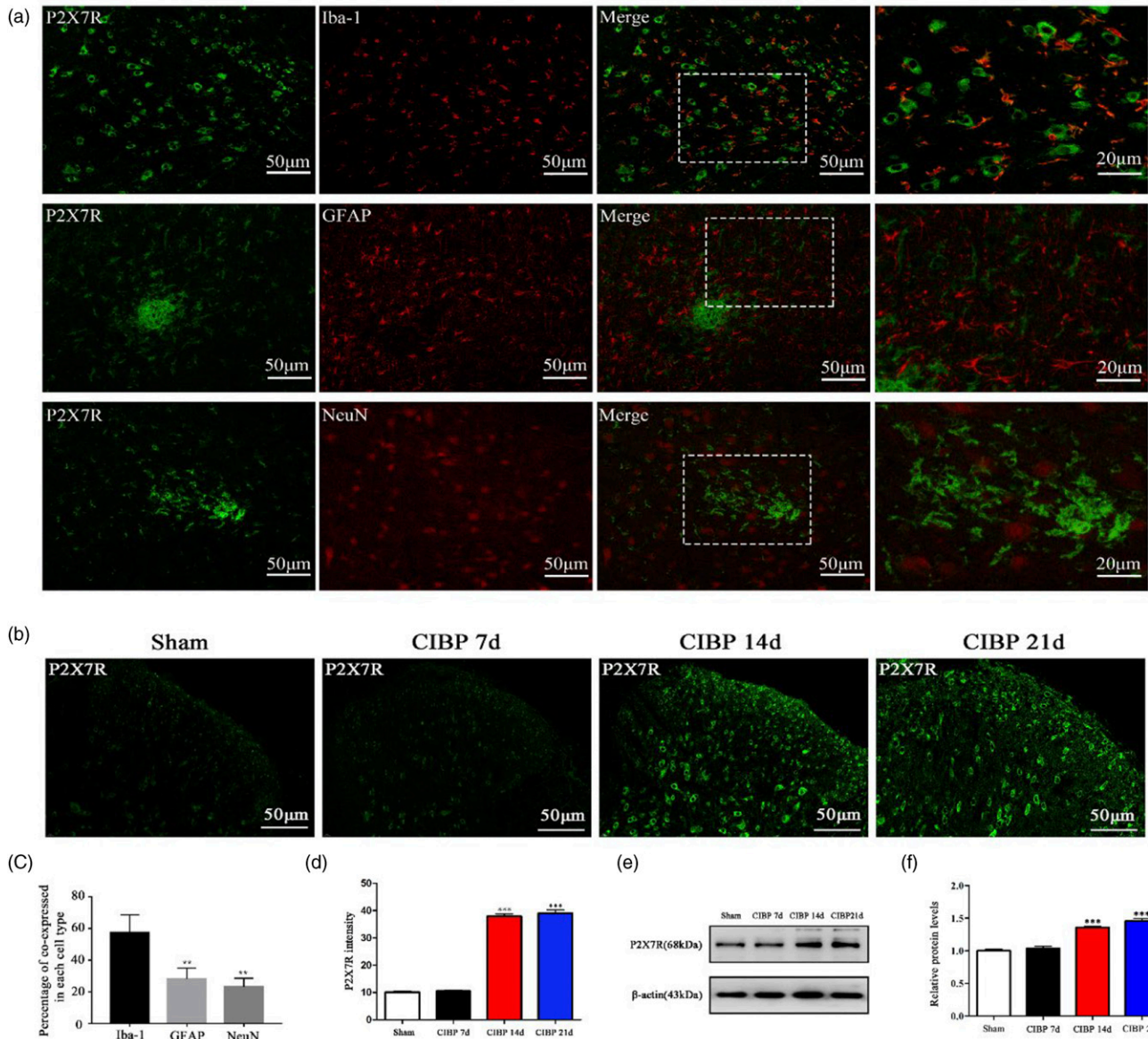


Figure 4. The expression of P2X7R have elevated in the CIBP group. (a) and (c) Co-immunostaining of P2X7R (green) and Iba-1 (microglial-specific marker, red) in the spinal dorsal horn of Sham rats and CIBP rats and the percentage of co-expressed in each cell type. $^{**}p < .01$ versus Iba-1. (b) and (d) Representative immunofluorescence image and quantitative data for analysis showed the P2X7R intensity in the Sham group and CIBP group on POD 7, 14, 21. Data were presented as mean \pm SD ($n = 4$ per group). $^{***}p < .001$ versus Sham group. (e) and (f) Representative Western blotting bands and quantitative data for analysis showed the protein expression levels of P2X7R in the Sham group and CIBP group on POD 7, 14, 21. β -actin was used as an internal control. Data were presented as mean \pm SD ($n = 4$ per group). $^{***}p < .001$ versus Sham group.

were performed to test the effects of BBG treatment on microglial polarization. Analysis showed that compared to NS, BBG significantly suppressed microglial polarization toward the M1 type in the CIBP group (Figure 5(c), (e), (f), (g), (h)). Besides, M2 type markers, CD163, Arg-1, IL-4, and IL-10 were significantly elevated in the CIBP+BBG group when compared to the CIBP+NS group (Figure 5(d), (i), (j), (k), (l)).

P2X7R siRNA inhibited BzATP-induced microglial polarization toward the M1 type and promoted microglial polarization toward the M2 type in BV2 cell lines

The BV-2 cells have a similar response to LPS stimulation as primary microglia and have been used in *in vitro* assays.²¹ Western blotting analysis was performed to determine the

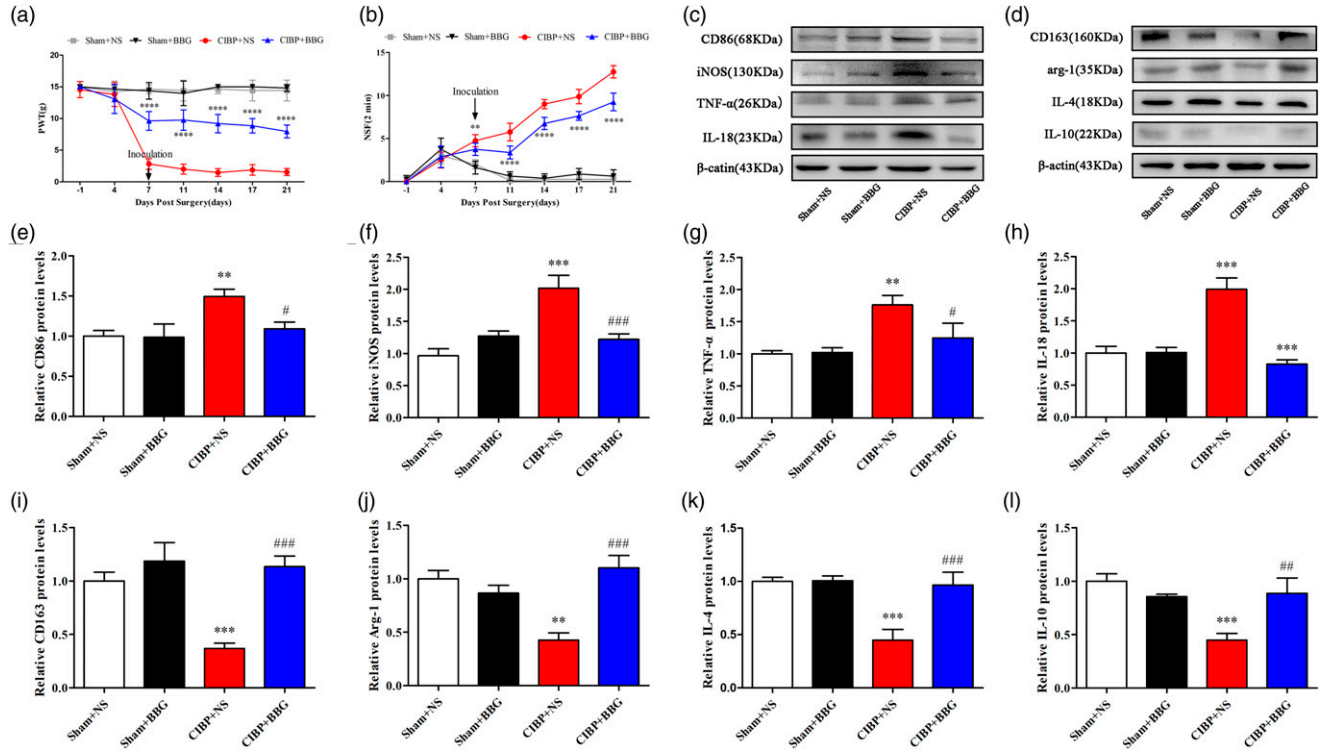


Figure 5. The P2X7R-specific inhibitor BBG can effectively alleviate CIBP and reduce the polarization of microglia to M1 type. (a) PWT in the Sham + NS, Sham + BBG, CIBP + NS, and CIBP + BBG group were examined on baseline (1 day before surgery) and POD 4, 7, 11, 14, 17, 21. Data were presented as mean \pm SD ($n = 8$ per group). $****p < .0001$ versus CIBP+NS group. (b) NSF in the Sham + NS, Sham + BBG, CIBP+NS, and CIBP+BBG group were examined on baseline (1 day before surgery) and POD 4, 7, 11, 14, 17, 21. Data were presented as mean \pm SD ($n = 8$ per group). $****p < .0001$ versus CIBP+NS group. (c), (e), (f), (g), (h) Representative Western blotting bands and quantitative analysis showed the protein expression levels of CD86, iNOS, TNF- α , and IL-18 in the Sham+NS, Sham+ BBG, CIBP+NS, and CIBP+BBG group. β -actin was used as an internal control. Data were presented as mean \pm SD ($n = 4$ per group). $*p < .01$ versus Sham+NS group; $***p < .001$ versus Sham+NS group; $\#p < .05$ versus CIBP+NS group; $####p < .001$ versus CIBP+NS group. (d), (i), (j), (k), (l) Representative Western blotting bands and quantitative analysis showed the protein expression levels of CD163, Arg-1, IL-4, and IL-10 in the Sham+NS, Sham+ BBG, CIBP+NS, and CIBP+BBG group. β -actin was used as an internal control. Data were presented as mean \pm SD ($n = 4$ per group). $*p < .01$ versus Sham+NS group; $***p < .001$ versus Sham+NS group; $\#p < .05$ versus CIBP+NS group; $####p < .001$ versus CIBP+NS group.

efficiency of transfection, then, P2X7siRNA3, which showed the highest silencing efficiency was selected (Supplementary File 2). BzATP, a synthetic agonist of ATP that binds the P2X receptor, revealed a higher potency relative to ATP in activating P2X7R.²² The experimental groups were stimulated for 30 min using 1 μ g/ml LPS, and the culture medium was discarded. Cells were then cultured in fresh medium supplemented with BzATP (300 μ M, # 112988-15-4, Sigma-Aldrich, Mo, USA) to establish a cell model of microglial activation. The activation model of BV2 cells and the timing of administration were derived from references.²³ Then, we investigated the impact of P2X7RsiRNA on activated BV2 cells. BzATP exposure significantly elevated the expression of M1 phenotypic markers, iNOS and CD86 as well as M1-type related inflammation-promoting factors, TNF- α and IL-18 (Figure 6(a), (b), (c), (g), (h)). However, expression levels of M2 phenotypic markers (CD163 and Arg-1) as well as M2-type related cytokines (IL-10 and IL-4) were suppressed (Figure 6(d), (e), (f), (i), (j)). Pretreatment with P2X7R siRNA reversed BzATP-induced changes in protein levels of CD86, iNOS,

CD163, Arg-1, while regulating TNF- α , IL-18, IL-4, and IL-10 mRNA expressions ($p < .05$). These findings imply that P2X7RsiRNA can suppress BzATP-induced microglial polarization toward the M1 type.

Discussion

CIBP is a complex state that is characterized by high neuropathic and inflammation-related pain as well as cancer-associated pain.²⁴ The specific mechanisms of CIBP have not been clearly elucidated. We inoculated Walker 256 rat breast cancer cells into the tibial cavity, thereby triggering mechanical allodynia, pathologic fracture, and osteolysis. These findings are consistent with those of previous studies.²⁵ This confirmed the accurate establishment of BCP rat models.

Inhibition of microglial polarization toward the M1 phenotype, or promotion of microglial polarization toward the M2 phenotype can relieve pain. Li et al.²⁶ reported that PPAR γ inhibits neuropathic pain by down-regulating CX3CR1 and

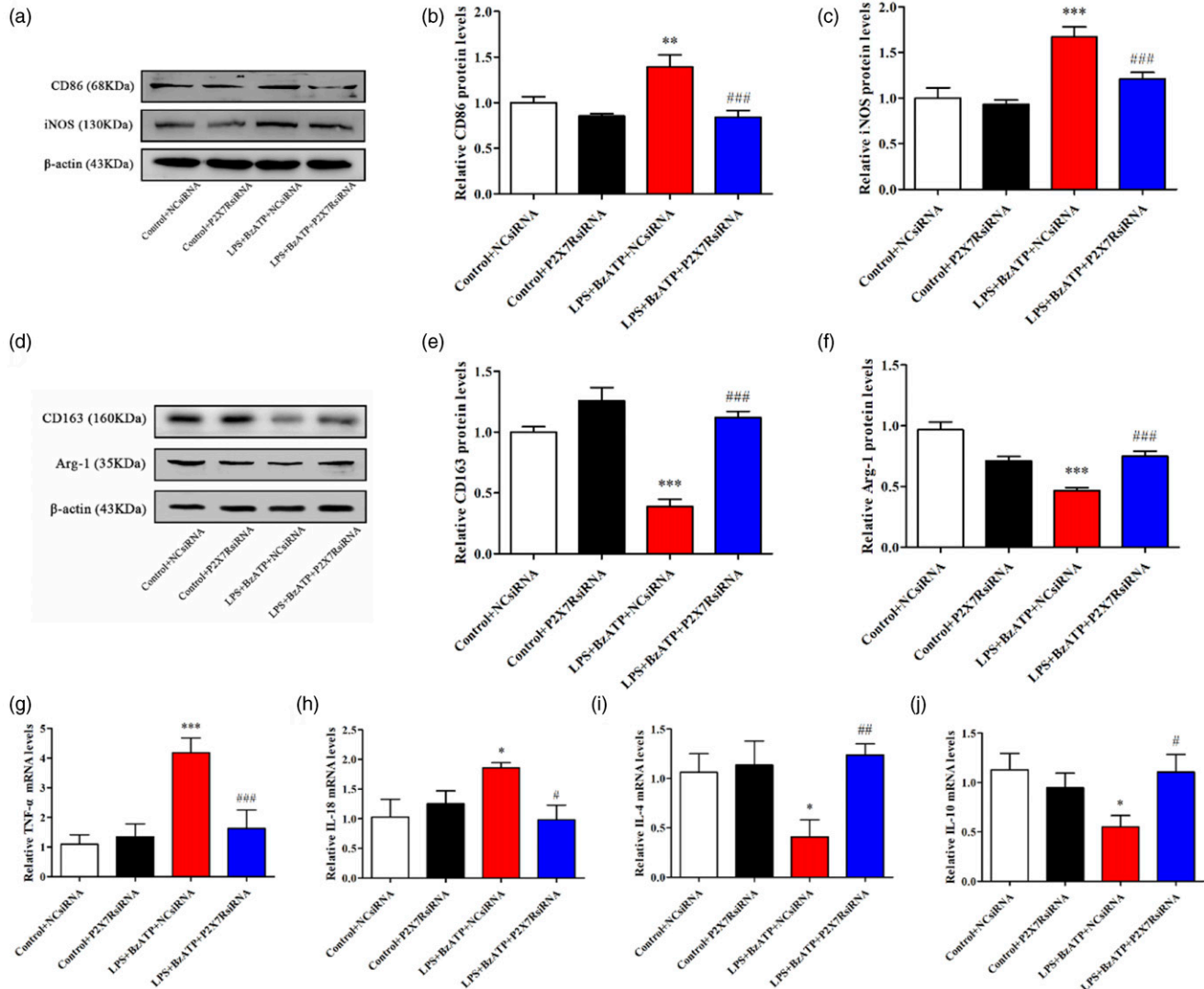


Figure 6. P2X7RsiRNA can reduce the polarization of microglia to M1 induced by BzATP. (a), (b), (c) Representative Western blotting bands and quantitative analysis showed the protein expression levels of CD86 and iNOS in the Control+NCsiRNA, Control+P2X7RsiRNA, LPS+BzATP+NCsiRNA, and LPS+BzATP+P2X7RsiRNA group. β -actin was used as an internal control. Data were presented as mean \pm SD ($n = 4$ per group). $^{*}p < .01$ versus Control+NCsiRNA group; $^{**}p < .001$ versus Control+NCsiRNA group; $^{###}p < .001$ versus LPS+BzATP+NCsiRNA group. (D), (E), (F) Representative Western blotting bands and quantitative analysis showed the protein expression levels of CD163 and Arg-1 in the Control+NCsiRNA, Control+P2X7RsiRNA, LPS+BzATP+NCsiRNA, and LPS+BzATP+P2X7RsiRNA group. β -actin was used as an internal control. Data were presented as mean \pm SD ($n = 4$ per group). $^{*}p < .001$ versus Control+NCsiRNA group; $^{###}p < .001$ versus LPS+BzATP+NCsiRNA group. (g), (h), (i), (j) Relative mRNA expression levels of IL-18, TNF- α , IL-4, and IL-10 in the Control+NCsiRNA, Control+P2X7RsiRNA, LPS+BzATP+NCsiRNA, and LPS+BzATP+P2X7RsiRNA group. Data were presented as mean \pm SD ($n = 4$ per group). $^{*}p < 0.05$ versus Control+NCsiRNA group; $^{**}p < 0.001$ versus Control+NCsiRNA group; $^{#}p < 0.05$ versus LPS+BzATP+NCsiRNA group; $^{###}p < 0.001$ versus LPS+BzATP+NCsiRNA group; $^{###}p < 0.001$ versus LPS+BzATP+NCsiRNA group.

suppressing M1 polarization of spinal microglia in rats. Jin et al.²⁷ showed that M2 polarization of microglia can improve Alzheimer's disease-associated neuropathic pain. We found that microglia is polarized toward the M1 phenotype in the spinal cords of CIBP rat models.

Besides, P2X7R has been shown to induce and maintain chronic pain.²⁸ Hu et al.²⁹ reported that intra-amygdala microinfusion of a P2X7R antagonist inhibits the activation of astrocytes and microglia and relieves neuropathic pain. Li et al.³⁰

reported that treatment with MiR-187-3p mimics alleviated pain hypersensitivity associated with ischemia-reperfusion-induced by suppressing P2X7R and reducing IL-1 β generation in the spinal cords of mice. However, the role of P2X7R in CIBP has not been explored. We found that P2X7R is highly expressed in the microglia, and the occurrence of CIBP reflects upregulation of P2X7R activation. Consistent with a previous study, our analysis demonstrated that a P2X7R-specific inhibitor, BBG, can effectively alleviate CIBP.³¹

Spinal microglia is involved in the development of chronic pain, including cancer-associated pain.³² Imbalanced microglial polarization promotes the development of neuroinflammatory damage.^{33,34} Recent studies have reported that P2X7R may be involved in microglial polarization. For instance, Gui et al.³⁵ reported that BTX-A promoted microglial M2 polarization and alleviated CCI-induced neuropathic pain by inhibiting the P2X7 receptor. Higashi et al.¹⁸ reported that the release of endogenous zinc was induced by cerebral ischemia-reperfusion, which activated microglial polarization toward M1 by activating the P2X7 receptor, and the release of inflammation-promoting cytokines, leading to deficits in object recognition memory. However, the roles of P2X7R in CIBP development have not been clearly elucidated. We found that elevated P2X7R levels induced spinal microglial transformation toward the M1 phenotype, accompanied by secretion of TNF- α and IL-18. Treatment with BBG, a P2X7R-specific antagonist, or P2X7RsiRNA, significantly elevated the expression levels of M2 phenotypic markers (CD163, Arg-1) and anti-inflammatory cytokines (IL-10, IL-4), while suppressing the expressions of M1 phenotypic markers (iNOS, CD86) and pro-inflammatory cytokines (TNF- α , IL-18), *in vivo* and *in vitro*. Systematic antagonism of TNF- α , IL-18

significantly alleviated tactile hypersensitivity and spontaneous bone cancer.³⁶ Besides, intrathecal injection of TNF- α can evoke pain hypersensitization, even in naive animals.³⁷ Expressions of IL-10 or IL-4 in microglia can induce mechanical allodynia in CIBP.^{38,39} Therefore, P2X7R is involved in modulation of microglial polarization toward the M1/M2 phenotypes.

Conclusion

P2X7R induces microglial polarization toward the M1 phenotype in cancer-induced bone pain rat models. Therefore, P2X7R is a potential therapeutic target for CIBP.

Supplemental result:

Supplementary Figure 1. Screening of P2X7R siRNA. (A) and (B) Representative Western blotting bands and quantitative analysis showed the protein expression levels of P2X7R in the NCsiRNA, P2X7RsiRNA1, P2X7RsiRNA2, P2X7RsiRNA3 group. β -actin was used as an internal control. Data were presented as mean \pm SD ($n = 4$ per group). ** $p < .01$ vs NCsiRNA group; ### $p < .01$ vs P2X7RsiRNA2 group.

Appendix

Notation

CIBP	cancer-induced bone pain
P2X7R	P2X7 receptor
PWT	Paw withdrawal thresholds
NSF	Number of spontaneous flinches
BBG	Brilliant blue G

Author contributions

P.W. and G.-H.Z. conducted the study and wrote the manuscript; X.-Q.W. performed pain behavioral tests, data collection and Western blotting; R.L. performed qRT-PCR analyses; J.-Q.Y. performed pathologic analyses; Q.-P.W. conceived the idea and designed the study. All authors reviewed and approved the final manuscript.

Declaration of conflicting interests

The author(s) declared no potential conflicts of interest with respect to the research, authorship, and/or publication of this article.

Funding

The author(s) received no financial support for the research, authorship, and/or publication of this article.

References

1. Yu J, Luo Y, Jin H, et al. Scorpion alleviates bone cancer pain through inhibition of bone destruction and glia activation. *Mol Pain* 2020; 16: 1744806920909993. DOI: [10.1177/1744806920909993](https://doi.org/10.1177/1744806920909993).
2. Harding D, Giles SL, Brown MRD, et al. Evaluation of quality of life outcomes following palliative treatment of bone metastases with magnetic resonance-guided high Intensity focused ultrasound: An international multicentre study. *Clin Oncol (R Coll Radiol)* 2018; 30: 233–242. DOI: [10.1016/j.clon.2017.12.023](https://doi.org/10.1016/j.clon.2017.12.023).
3. Yang B, Zhang Z, Yang Z, et al. Chanling gao attenuates bone cancer pain in rats by the IKK β /NF- κ B signaling pathway. *Front Pharmacol* 2020; 11: 525. DOI: [10.3389/fphar.2020.00525](https://doi.org/10.3389/fphar.2020.00525).
4. Currie GL, Delaney A, Bennett MI, et al. Animal models of bone cancer pain: systematic review and meta-analyses. *Pain* 2013; 154: 917–926. DOI: [10.1016/j.pain.2013.02.033](https://doi.org/10.1016/j.pain.2013.02.033).
5. Cai J, Fang D, Liu XD, et al. Suppression of KCNQ/M (Kv7) potassium channels in the spinal cord contributes to the sensitization of dorsal horn WDR neurons and pain hypersensitivity in a rat model of bone cancer pain. *Oncol Rep* 2015; 33: 1540–1550. DOI: [10.3892/or.2015.3718](https://doi.org/10.3892/or.2015.3718).
6. Hua B, Gao Y, Kong X, et al. New insights of nociceptor sensitization in bone cancer pain. *Expert Opin Ther Targets* 2015; 19: 227–243. DOI: [10.1517/14728222.2014.980815](https://doi.org/10.1517/14728222.2014.980815).
7. Tang Y, Liu L, Xu D, et al. Interaction between astrocytic colony stimulating factor and its receptor on microglia mediates central sensitization and behavioral hypersensitivity in chronic post ischemic pain model. *Brain Behav Immun* 2018; 68: 248–260. DOI: [10.1016/j.bbi.2017.10.023](https://doi.org/10.1016/j.bbi.2017.10.023).

8. Zhang J, Zheng Y, Luo Y, et al. Curcumin inhibits LPS-induced neuroinflammation by promoting microglial M2 polarization via TREM2/TLR4/NF- κ B pathways in BV2 cells. *Mol Immunol* 2019; 116: 29–37. DOI: [10.1016/j.molimm.2019.09.020](https://doi.org/10.1016/j.molimm.2019.09.020).
9. Zhao R, Ying M, Gu S, et al. Cysteinyl leukotriene receptor 2 is involved in inflammation and neuronal damage by mediating microglia M1/M2 polarization through NF- κ B pathway. *Neuroscience* 2019; 422: 99–118. DOI: [10.1016/j.neuroscience.2019.10.048](https://doi.org/10.1016/j.neuroscience.2019.10.048).
10. Wu HY, Tang XQ, Mao XF, et al. Autocrine interleukin-10 mediates glucagon-like peptide-1 receptor-induced spinal microglial β -endorphin expression. *J Neurosci* 2017; 37: 11701–11714. DOI: [10.1523/jneurosci.1799-17.2017](https://doi.org/10.1523/jneurosci.1799-17.2017).
11. Zhu MD, Zhao LX, Wang XT, et al. Ligustilide inhibits microglia-mediated proinflammatory cytokines production and inflammatory pain. *Brain Res Bull* 2014; 109: 54–60. DOI: [10.1016/j.brainresbull.2014.10.002](https://doi.org/10.1016/j.brainresbull.2014.10.002).
12. Jiang Y, Wang J, Li H, et al. IL-35 promotes microglial M2 polarization in a rat model of diabetic neuropathic pain. *Arch Biochem Biophys* 2020; 685: 108330. DOI: [10.1016/j.abb.2020.108330](https://doi.org/10.1016/j.abb.2020.108330).
13. Bartlett R, Yerbury JJ, Sluyter R. P2X7 receptor activation induces reactive oxygen species formation and cell death in murine EOC13 microglia. *Mediators Inflamm* 2013; 2013: 271813. DOI: [10.1155/2013/271813](https://doi.org/10.1155/2013/271813).
14. He Y, Taylor N, Fourgeaud L, et al. The role of microglial P2X7: modulation of cell death and cytokine release. *J Neuroinflammation* 2017; 14: 135. DOI: [10.1186/s12974-017-0904-8](https://doi.org/10.1186/s12974-017-0904-8).
15. Bhattacharya A, Biber K. The microglial ATP-gated ion channel P2X7 as a CNS drug target. *Glia* 2016; 64: 1772–1787. DOI: [10.1002/glia.23001](https://doi.org/10.1002/glia.23001).
16. Huang ZX, Lu ZJ, Ma WQ, et al. Involvement of RVM-expressed P2X7 receptor in bone cancer pain: mechanism of descending facilitation. *Pain* 2014; 155: 783–791. DOI: [10.1016/j.pain.2014.01.011](https://doi.org/10.1016/j.pain.2014.01.011).
17. Chessell IP, Hatcher JP, Bountra C, et al. Disruption of the P2X7 purinoceptor gene abolishes chronic inflammatory and neuropathic pain. *Pain* 2005; 114: 386–396. DOI: [10.1016/j.pain.2005.01.002](https://doi.org/10.1016/j.pain.2005.01.002).
18. Higashi Y, Aratake T, Shimizu S, et al. Influence of extracellular zinc on M1 microglial activation. *Sci Rep* 2017; 7: 43778. DOI: [10.1038/srep43778](https://doi.org/10.1038/srep43778).
19. Song J, Ying Y, Wang W, et al. The role of P2X7R/ERK signaling in dorsal root ganglia satellite glial cells in the development of chronic postsurgical pain induced by skin/muscle incision and retraction (SMIR). *Brain Behav Immun* 2018; 69: 180–189. DOI: [10.1016/j.bbi.2017.11.011](https://doi.org/10.1016/j.bbi.2017.11.011).
20. Zhou YQ, Liu Z, Liu HQ, et al. Targeting glia for bone cancer pain. *Expert Opin Ther Targets* 2016; 20: 1365–1374. DOI: [10.1080/14728222.2016.1214716](https://doi.org/10.1080/14728222.2016.1214716).
21. Raouf R, Chabot-Doré AJ, Ase AR, et al. Differential regulation of microglial P2X4 and P2X7 ATP receptors following LPS-induced activation. *Neuropharmacology* 2007; 53: 496–504. DOI: [10.1016/j.neuropharm.2007.06.010](https://doi.org/10.1016/j.neuropharm.2007.06.010).
22. Asatryan L, Ostrovskaya O, Lieu D, et al. Ethanol differentially modulates P2X4 and P2X7 receptor activity and function in BV2 microglial cells. *Neuropharmacology* 2018; 128: 11–21. DOI: [10.1016/j.neuropharm.2017.09.030](https://doi.org/10.1016/j.neuropharm.2017.09.030).
23. Rampe D, Wang L, Ringheim GE. P2X7 receptor modulation of beta-amyloid- and LPS-induced cytokine secretion from human macrophages and microglia. *J Neuroimmunol* 2004; 147: 56–61. DOI: [10.1016/j.jneuroim.2003.10.014](https://doi.org/10.1016/j.jneuroim.2003.10.014).
24. Falk S, Dickenson AH. Pain and nociception: mechanisms of cancer-induced bone pain. *J Clin Oncol* 2014; 32: 1647–1654. DOI: [10.1200/jco.2013.51.7219](https://doi.org/10.1200/jco.2013.51.7219).
25. Yang B, Zhang Z, Yang Z, et al. Chanling gao attenuates bone cancer pain in rats by the IKK β /NF- κ B signaling pathway. *Front Pharmacol* 2020; 11: 525. DOI: [10.3389/fphar.2020.00525](https://doi.org/10.3389/fphar.2020.00525).
26. Li X, Guo Q, Ye Z, et al. PPAR γ prevents Neuropathic pain by down-regulating CX3CR1 and attenuating M1 activation of microglia in the spinal cord of rats using a sciatic chronic constriction injury model. *Front Neurosci* 2021; 15: 620525. DOI: [10.3389/fnins.2021.620525](https://doi.org/10.3389/fnins.2021.620525).
27. Jin J, Guo J, Cai H, et al. M2-like microglia polarization attenuates neuropathic pain associated with Alzheimer's disease. *J Alzheimers Dis* 2020; 76: 1255–1265. DOI: [10.3233/JAD-200099](https://doi.org/10.3233/JAD-200099).
28. Bernier LP, Ase AR, Séguéla P. P2X receptor channels in chronic pain pathways. *Br J Pharmacol* 2018; 175: 2219–2230. DOI: [10.1111/bph.13957](https://doi.org/10.1111/bph.13957).
29. Hu X, Liu Y, Wu J, et al. Inhibition of P2X7R in the amygdala ameliorates symptoms of neuropathic pain after spared nerve injury in rats. *Brain Behav Immun* 2020; 88: 507–514. DOI: [10.1016/j.bbi.2020.04.030](https://doi.org/10.1016/j.bbi.2020.04.030).
30. Li XQ, Yu Q, Zhang ZL, et al. MiR-187-3p mimic alleviates ischemia-reperfusion-induced pain hypersensitivity through inhibiting spinal P2X7R and subsequent mature IL-1 β release in mice. *Brain Behav Immun* 2019; 79: 91–101. DOI: [10.1016/j.bbi.2019.05.021](https://doi.org/10.1016/j.bbi.2019.05.021).
31. Yang Y, Li H, Li TT, et al. Delayed activation of spinal microglia contributes to the maintenance of bone cancer pain in female Wistar rats via P2X7 receptor and IL-18. *J Neurosci* 2015; 35: 7950–7963. DOI: [10.1523/JNEUROSCI.5250-14.2015](https://doi.org/10.1523/JNEUROSCI.5250-14.2015).
32. Tamagawa T, Shinoda M, Honda K, et al. Involvement of microglial P2Y12 signaling in tongue cancer pain. *J Dent Res* 2016; 95: 1176–1182. DOI: [10.1177/0022034516647713](https://doi.org/10.1177/0022034516647713).
33. Yao K, Zu HB. Microglial polarization: novel therapeutic mechanism against Alzheimer's disease. *Inflammopharmacology* 2020; 28: 95–110. DOI: [10.1007/s10787-019-00613-5](https://doi.org/10.1007/s10787-019-00613-5).
34. Xiong XY, Liu L, Yang QW. Functions and mechanisms of microglia/macrophages in neuroinflammation and neurogenesis after stroke. *Prog Neurobiol* 2016; 142: 23–44. DOI: [10.1016/j.pneurobio.2016.05.001](https://doi.org/10.1016/j.pneurobio.2016.05.001).
35. Gui X, Wang H, Wu L, et al. Botulinum toxin type A promotes microglial M2 polarization and suppresses chronic constriction

- injury-induced neuropathic pain through the P2X7 receptor. *Cell Biosci* 2020; 10: 45. DOI: [10.1186/s13578-020-00405-3](https://doi.org/10.1186/s13578-020-00405-3).
36. Geis C, Graulich M, Wissmann A, et al. Evoked pain behavior and spinal glia activation is dependent on tumor necrosis factor receptor 1 and 2 in a mouse model of bone cancer pain. *Neuroscience* 2010; 169: 463–474. DOI: [10.1016/j.neuroscience.2010.04.022](https://doi.org/10.1016/j.neuroscience.2010.04.022).
 37. Gao YJ, Zhang L, Ji RR. Spinal injection of TNF- α -activated astrocytes produces persistent pain symptom mechanical allodynia by releasing monocyte chemoattractant protein-1. *Glia* 2010; 58: 1871–1880. DOI: [10.1002/glia.21056](https://doi.org/10.1002/glia.21056).
 38. Grenald SA, Doyle TM, Zhang H, et al. Targeting the SIP/S1PR1 axis mitigates cancer-induced bone pain and neuroinflammation. *Pain* 2017; 158: 1733–1742. DOI: [10.1097/j.pain.0000000000000965](https://doi.org/10.1097/j.pain.0000000000000965).
 39. Wang Y, Ni H, Li H, et al. Nuclear factor kappa B regulated monocyte chemoattractant protein-1/chemokine CC motif receptor-2 expressing in spinal cord contributes to the maintenance of cancer-induced bone pain in rats. *Mol Pain* 2018; 14: 1744806918788681. DOI: [10.1177/1744806918788681](https://doi.org/10.1177/1744806918788681).